



**HAL**  
open science

## Zonotopic set-membership state estimation applied to an octorotor model

Dory Merhy, Cristina Stoica Maniu, Teodoro Alamo, Eduardo Fernandez  
Camacho, Thomas Chevet, Maria Makarov, Israël Hinostroza

► **To cite this version:**

Dory Merhy, Cristina Stoica Maniu, Teodoro Alamo, Eduardo Fernandez Camacho, Thomas Chevet, et al.. Zonotopic set-membership state estimation applied to an octorotor model. 12th Summer Workshop on Interval Methods, Jul 2019, Palaiseau, France. hal-02275035

**HAL Id: hal-02275035**

**<https://hal.science/hal-02275035>**

Submitted on 30 Aug 2019

**HAL** is a multi-disciplinary open access archive for the deposit and dissemination of scientific research documents, whether they are published or not. The documents may come from teaching and research institutions in France or abroad, or from public or private research centers.

L'archive ouverte pluridisciplinaire **HAL**, est destinée au dépôt et à la diffusion de documents scientifiques de niveau recherche, publiés ou non, émanant des établissements d'enseignement et de recherche français ou étrangers, des laboratoires publics ou privés.

# Zonotopic set-membership state estimation applied to an octorotor model

Dory Merhy<sup>\*1</sup>, Cristina Stoica Maniu<sup>1</sup>, Teodoro Alamo<sup>2</sup>, Eduardo F. Camacho<sup>2</sup>, Thomas Chevet<sup>1</sup>, Maria Makarov<sup>1</sup>, and Israel Hinostroza<sup>3</sup>

<sup>1</sup>Laboratoire des Signaux et Systèmes (L2S), CentraleSupélec-CNRS-Université Paris-Sud, Université Paris-Saclay, 3 rue Joliot Curie, F-91192, Gif-sur-Yvette, France

<sup>2</sup>Department of Ingeniería de Sistemas y Automática, Universidad de Sevilla, Camino de los Descubrimientos, 41092 Sevilla, Spain

<sup>3</sup>SONDRA Lab, CentraleSupélec, 3 rue Joliot-Curie, 91192 Gif-sur-Yvette, France

**Keywords:** Set-membership state estimation, Octorotor, Linear Matrix Inequality

## Introduction

In control systems, state estimators are mainly used to filter redundant data, to eliminate erroneous measurements and to produce reliable state estimations in the presence of measurement noises and perturbations. In 1960, Kalman set the ground for a new class of state estimation techniques by introducing his famous powerful yet simple filter, that considers known (Gaussian) distributions of measurement noises and state perturbations. Sometimes, the assumptions that the classical filter uses are not too realistic. Therefore, as an alternative, the deterministic approaches arose by considering unknown but bounded perturbations and measurement noises. Among this family, a particular interesting approach is the set-membership state estimation, where different sets can be used. The choice of the considered set mainly depends on the application and on the trade-off between accuracy and simplicity. However, despite the precision and the low complexity that some set-membership state estimation techniques can offer, there is still a gap between theory and practice in this field. In this context, few set-membership state estimators were tested on new technologies, in particu-

lar on Unmanned Aerial Vehicles (UAVs) [2], [6] and robots [3], or extended to incorporate physical state constraints [5]. In this work, a zonotopic set-membership state estimation technique is applied to the position estimation of an octorotor model used for radar applications. The model complexity and the perturbations coming from different sources make the state estimation of the drone a challenging problem. In this case, an accurate position estimation of the UAV is needed for the radar to provide high resolution images.

## Zonotopic set-membership state estimation technique

Consider the following detectable discrete-time linear time invariant system:

$$\begin{aligned}\mathbf{x}_{k+1} &= \mathbf{A}\mathbf{x}_k + \mathbf{B}\mathbf{u}_k + \mathbf{E}\boldsymbol{\omega}_k \\ \mathbf{y}_k &= \mathbf{C}\mathbf{x}_k + \mathbf{F}\boldsymbol{\omega}_k\end{aligned}\quad (1)$$

with  $\mathbf{x}_k \in \mathbb{R}^{n_x}$ ,  $\mathbf{u}_k \in \mathbb{R}^{n_u}$ ,  $\mathbf{y}_k \in \mathbb{R}^{n_y}$ , and  $\boldsymbol{\omega}_k$  belonging to the unitary box  $\mathbb{B}^{n_x+n_y}$ .

**Theorem 1.** (based on [7]) Consider  $\mathbf{x}_0$  and assume that the state  $\mathbf{x}_k$  belongs to the zonotope  $\mathcal{Z}(\mathbf{p}_k, \mathbf{H}_k) = \mathbf{p}_k \oplus \mathbf{H}_k \mathbb{B}^m$ . Given a scalar  $\beta \in (0, 1)$ , if there exist a positive definite matrix  $\mathbf{P} = \mathbf{P}^\top \succ 0$  in  $\mathbb{R}^{n_x \times n_x}$  and a matrix  $\mathbf{Y} \in \mathbb{R}^{n_x \times n_y}$  for which the following linear matrix inequality (LMI) holds

$$\begin{bmatrix} \beta \mathbf{P} & 0 & \mathbf{A}^\top \mathbf{P} - \mathbf{C}^\top \mathbf{Y}^\top \\ * & \mathbf{T}^\top \mathbf{T} & \mathbf{E}^\top \mathbf{P} - \mathbf{F}^\top \mathbf{Y}^\top \\ * & * & \mathbf{P} \end{bmatrix} \succeq 0 \quad (2)$$

<sup>\*</sup>Corresponding author.

then it is guaranteed that  $\mathbf{x}_{k+1} \in \mathcal{Z}(\bar{\mathbf{x}}_{k+1}, \mathbf{H}_{k+1})$ ,  $\forall \boldsymbol{\omega}_k \in \mathbb{B}^{n_x+n_y}$ , where:

$$\bar{\mathbf{x}}_{k+1} = \mathbf{A}\bar{\mathbf{x}}_k + \mathbf{B}\mathbf{u}_k + \mathbf{L}(y_k - \mathbf{C}\bar{\mathbf{x}}_k) \quad (3)$$

$$\mathbf{H}_{k+1} = [\mathbf{A}_L \mathbf{H}_k \quad \boldsymbol{\eta}] \quad (4)$$

with  $\mathbf{Y} = \mathbf{P}\mathbf{L}$ ,  $\mathbf{T} = [\mathbf{E}^\top \quad \mathbf{F}^\top]^\top$ ,  $\mathbf{A}_L = \mathbf{A} - \mathbf{L}\mathbf{C}$  and  $\boldsymbol{\eta} = \mathbf{E} - \mathbf{L}\mathbf{F}$ .

**Sketch of proof:** The error  $\mathbf{z}_k = \mathbf{x}_k - \bar{\mathbf{x}}_k$  between the real state and the nominal estimated state at time  $k$  belongs to the centered zonotope  $\mathbf{H}_k \mathbb{B}^m$ . At time  $k+1$ , one has  $\mathbf{z}_{k+1} = \mathbf{A}_L \mathbf{z}_k + \boldsymbol{\eta} \boldsymbol{\omega}_k \in \mathbf{H}_{k+1} \mathbb{B}^{m+n_x+n_y}$ .

The non increase of the P-radius [4] of the zonotopic error can be expressed such that  $\max_{\hat{\mathbf{z}}} \|\mathbf{H}_{k+1} \hat{\mathbf{z}}\|_{\mathbf{P}}^2 \leq \beta \max_{\mathbf{z}} \|\mathbf{H}_k \mathbf{z}\|_{\mathbf{P}}^2 + \max_{\mathbf{t}} \|\mathbf{T}\mathbf{t}\|_2^2$

with the notations  $\hat{\mathbf{z}} = [\mathbf{z}^\top \quad \mathbf{t}^\top]^\top \in \mathbb{B}^{m+n_x+n_y}$ ,  $\mathbf{z} \in \mathbb{B}^m$  and  $\mathbf{t} \in \mathbb{B}^{n_x+n_y}$ .

Using the reverse triangle inequality leads to a sufficient condition for  $\max_{\hat{\mathbf{z}}} (\|\mathbf{H}_{k+1} \hat{\mathbf{z}}\|_{\mathbf{P}}^2 - \beta \|\mathbf{H}_k \mathbf{z}\|_{\mathbf{P}}^2 - \|\mathbf{T}\mathbf{t}\|_2^2) \leq 0$ . Extensively,  $\forall \mathbf{z}, \mathbf{t}$ , the next expression is verified

$$\hat{\mathbf{z}}^\top \mathbf{H}_{k+1}^\top \mathbf{P} \mathbf{H}_{k+1} \hat{\mathbf{z}} - \beta \mathbf{z}^\top \mathbf{H}_k \mathbf{P} \mathbf{H}_k \mathbf{z} - \mathbf{t}^\top \mathbf{T}^\top \mathbf{T} \mathbf{t} \leq 0 \quad (5)$$

Replacing  $\mathbf{H}_{k+1} \hat{\mathbf{z}} = (\mathbf{A} - \mathbf{L}\mathbf{C})\mathbf{H}_k \mathbf{z} + (\mathbf{E} - \mathbf{L}\mathbf{F})\mathbf{t}$  in Eq. (5) and using the Schur complement lead us to the LMI (2).

## Octorotor modeling

The Mikrokopter ARF Okto-XL is equipped with a micro-controller that provides fused and filtered information from the sensors about the drone's position. A non-linear dynamical model together with a linearized model around the static hovering equilibrium with null translational and rotational velocities and null roll, pitch and yaw angles exist [1]. The linearized model [1] can be decoupled into three double integrator subsystems and then discretized with a sampling period  $T_s$ . However, for linear position estimation problems, we only need the two subsystems describing the longitudinal and the altitude dynamics, respectively:

$$\begin{aligned} \mathbf{x}_{1_{k+1}} &= \mathbf{A}\mathbf{x}_{1_k} + \mathbf{B}_1 \mathbf{u}_{1_k} + \mathbf{E}_1 \boldsymbol{\omega}_k \\ \mathbf{y}_{1_k} &= \mathbf{C}\mathbf{x}_{1_k} + \mathbf{F}_1 \boldsymbol{\omega}_k \end{aligned} \quad (6)$$

$$\begin{aligned} \mathbf{x}_{3_{k+1}} &= \mathbf{A}\mathbf{x}_{3_k} + \mathbf{B}_3 \mathbf{u}_{3_k} + \mathbf{E}_3 \boldsymbol{\omega}_k \\ \mathbf{y}_{3_k} &= \mathbf{C}\mathbf{x}_{3_k} + \mathbf{F}_3 \boldsymbol{\omega}_k \end{aligned} \quad (7)$$

with  $\mathbf{x}_{1_k} = [z_k \quad \psi_k \quad V_{z_k} \quad \omega_{z_k}]^\top$ ,  $\mathbf{x}_{3_k} = [x_k \quad y_k \quad V_{x_k} \quad V_{y_k}]^\top$ ,  $\mathbf{u}_{1_k} = [F_{z_k}^R \quad \tau_{z_k}^R]^\top$ ,  $\mathbf{u}_{3_k} = [F_{x_k}^R \quad F_{y_k}^R]^\top$ ,  $\mathbf{y}_{1_k} = [z_k \quad \psi_k]^\top$ ,  $\mathbf{y}_{3_k} = [x_k \quad y_k]^\top$ ,  $\mathbf{A} = \begin{bmatrix} I_2 & T_s I_2 \\ 0_2 & I_2 \end{bmatrix}$ ,  $\mathbf{B}_1 =$

$$\begin{bmatrix} 0 & 0 \\ 0 & 0 \\ \frac{T_s}{m} & 0 \\ 0 & \frac{T_s}{I_{zz}} \end{bmatrix}, \mathbf{B}_3 = \begin{bmatrix} 0 & 0 \\ 0 & 0 \\ \frac{T_s}{m} & 0 \\ 0 & \frac{T_s}{m} \end{bmatrix}, \mathbf{C} = [I_2 \quad 0_2].$$

The notations and parameter values are detailed in [1]. Furthermore, the perturbations and the measurement noises  $\boldsymbol{\omega}_k$  are bounded by the unitary box  $\mathbb{B}^6$ . Additionally,  $\mathbf{E}_i = \epsilon_i \cdot [I_4 \quad 0_{4 \times 2}]$ ,  $\mathbf{F}_i = \gamma_i \cdot [0_4 \quad I_{4 \times 2}]$ , for  $i \in \{1, 3\}$ , with  $\epsilon_i$  and  $\gamma_i$  two scalars representing the accuracy provided by the drone sensors. The control inputs  $F_x^R$ ,  $F_y^R$  and  $F_z^R$  are the components of the resulting propeller's force, whereas  $\tau_z^R$  is the component of the resulting propeller's torque expressed in the drone's frame denoted by the superscript  $R$ .

## Simulation results

The highest sampling period  $T_s = 0.02$ s of all sensors is considered. The systems are fully controllable and observable. Based on the GPS, altimeter and gyroscope information, the following values are considered for  $\gamma_1 = \gamma_3 = 1$  and  $\epsilon_1 = \epsilon_3 = 10^{-3}$ . The UAV mass is 3.69kg and the inertia component  $I_{zz}$  w.r.t. to the z-axis is 0.0869kg·m<sup>2</sup>. The drone's behavior was tested using a Matlab/Simulink simulator implementing the non-linear model with a linear quadratic integral (LQI) controller [1] for which the nominal control inputs are then fed into the linear designed system. A linear trajectory is simulated to validate the efficiency of the zonotopic set-membership esti-

mation technique. It corresponds to a take-off to an altitude of 50m and then to a flight on the x-axis with a linear constant speed. The flight duration is 235s.

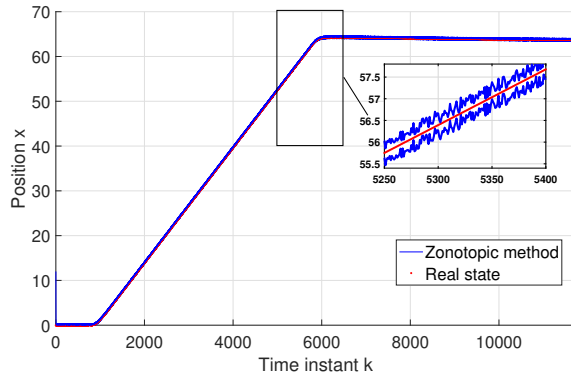


Figure 1: Bounds of the linear position  $x$

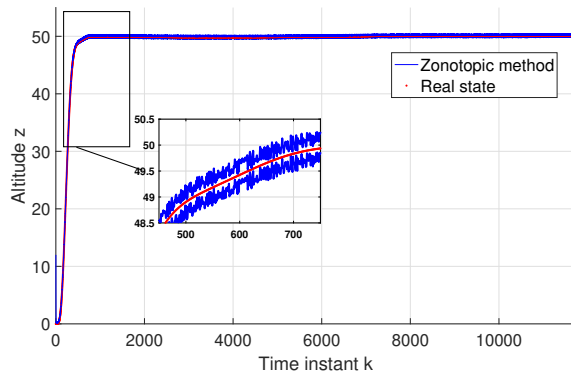


Figure 2: Bounds of the altitude  $z$

Figure 1 shows the zonotopic bounds (in blue) of the linear position  $x$  of the drone, whereas Figure 2 presents the guaranteed estimation bounds (in blue) of the altitude  $z$ . The real state (in red) in both cases lies inside the bounds despite of the considered measurement noises and state perturbations.

## Conclusion

A guaranteed zonotopic set-membership state estimation technique has been considered to compute the guaranteed linear position bounds of an octorotor model.

## Acknowledgement

The authors acknowledge MINERCO, FEDER funds, and EU Programme H2020 for funding projects DPI2016-76493-C3-1-R and SI-1838/24/2018.

## References

- [1] T. Chevet, M. Makarov, C. Stoica Maniu, I. Hinostroza, and P. Tarascon. State estimation of an octorotor with unknown inputs. Application to radar imaging. *21st ICSTCC*, 2017.
- [2] R. A. Garcia, G. V. Raffo, M. G. Ortega, and F. R. Rubio. Guaranteed quadrotor position estimation based on GPS refreshing measurements. *1st IFAC Workshop on Advanced Control and Navigation for Autonomous Aerospace Vehicles*, 48(9), 2015.
- [3] L. Jaulin. Robust set-membership state estimation; application to underwater robotics. *Automatica*, 45, 2009.
- [4] V. T. H. Le, C. Stoica, T. Alamo, E. Camacho, and D. Dumur. Zonotopic guaranteed state estimation for uncertain systems. *Automatica*, 49, 2013.
- [5] D. Merhy, T. Alamo, C. Stoica Maniu, and E. F. Camacho. Zonotopic constrained Kalman filter based on a dual formulation. In *IEEE CDC*, 2018.
- [6] G. Rousseau, C. Stoica Maniu, S. Tebbani, M. Babel, and N. Martin. Minimum-time B-spline trajectories with corridor constraints. Application to cinematographic quadrotor flight plans. *Control Engineering Practice*, 89, 2019.
- [7] Y. Wang, V. Puig, and G. Cembrano. Set-membership approach and Kalman observer based on zonotopes for discrete-time descriptor systems. *Automatica*, 93, 2018.